Mechanism and Machine Theory 114 (2017) 60–73

Contents lists available at ScienceDirect

Mechanism and Machine Theory

journal homepage: www.elsevier.com/locate/mechmachtheory

Research paper

Manufacturing and contact characteristics analysis of internal straight beveloid gear pair

Qilin Chen, Chaosheng Song*, Caichao Zhu, Xuesong Du, Gaoxiang Ni

The State Key Laboratory of Mechanical Transmissions, Chongqing University, Chongqing 400030, PR China

ARTICLE INFO

Article history:
Received 16 November 2016
Revised 14 March 2017
Accepted 4 April 2017

Keywords:
Internal straight beveloid gear
Manufacturing method
Mesh model
Loaded tooth contact analysis
Contact characteristics

ABSTRACT

This paper presents a manufacturing method for straight internal beveloid gear pair by shaper cutter with parallel axes between the cutter and the gear blank. The cutting motions are represented using three degrees of freedom that are the rotation along its axes, translations along the axial and radial directions. With the proposed method, the beveloid gear with a linear or nonlinear variable profile shift coefficient along the tooth width direction can be generated and the tilt deviations by the inclined cutting tool shaft can be avoided. The mathematical description of shaper cutter and the coordinate systems for the cutting procedure were defined. And the mathematical model of external and internal beveloid gears were derived and the loaded tooth contact analysis were conducted. Results show that the teeth mesh in at the toe and mesh out at the heel. The length of the simultaneous contact line on tooth surface increases first and then decreases due to the cone angle. As the load increases, the mesh area, contact pressure, mean value of mesh stiffness and the peak-peak value of angular transmission error are increased due to the elastic deformation. However, the speeds of the increase tendency slow down.

1. Introduction

Beveloid gears which was first proposed by Mettitt in 1954 [1] becomes an important gear drive for power and motion transmission due to their advantages, such as abilities to backlash control, misalignments absorption and easy manufacturing. For its conical shape with variable addendum modification along their tooth width, beveloid gearing can be installed with parallel, intersected and crossed axes. Internal gear pairs are widely used in reduction gear systems with their high gear ratio and small space requirement. Also, internal beveloid gears have smaller relative sliding speed on tooth surface and higher bearing capacity of tooth surface compared with the external beveloid gear transmission [2]. In the last couple of decades, a number of studies have been performed on the external beveloid gearing theory, design, manufacturing and tooth contact analysis. Unfortunately, little work can be found for the internal beveloid gearing theory and design.

Recently, there has been some efforts made to widen the application of beveloid gear drive [3–9]. Mitome investigated the geometry design of the nonintersecting-nonparallel-axis beveloid gear and two design methods were proposed with and without mounting dimensions [10]. Brauer theoretically analyzed the parameters of straight beveloid gears from a geometric point of view [11]. Wu and Tsai designed the beveloid gears to realize single tooth surface approximate line contact [12] and analyzed the contact characteristics of the tooth surface for crossed beveloid gear pair [13]. Hori proposed a synthesis method for tooth profiles using vector equations to precisely derive the curve of tooth profile of conical-external and

* Corresponding author.
E-mail address: chaoshengsong@cqu.edu.cn (C. Song).

http://dx.doi.org/10.1016/j.mechmachtheory.2017.04.002
0094-114X/

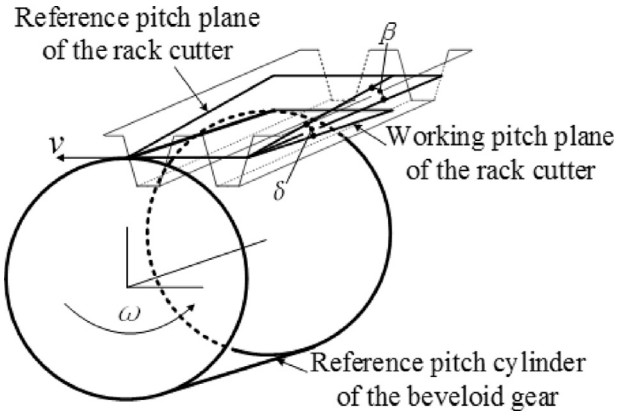

Fig. 1. External beveloid gear manufactured by an imaginary planar rack cutter [18,19].

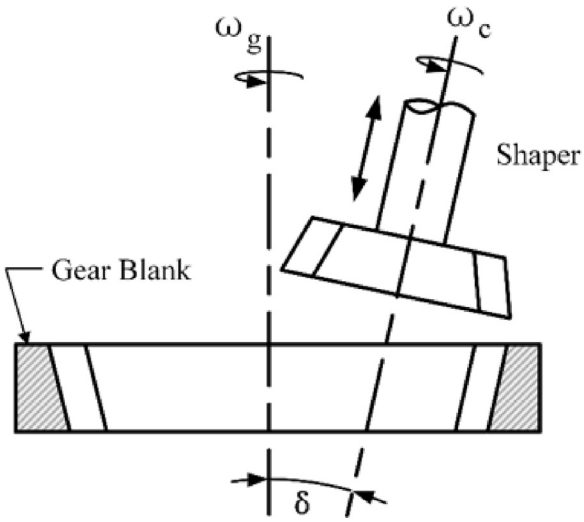

Fig. 2. Internal straight beveloid gears manufactured by cutter shaper [20].

conical-internal gears which engage a cylindrical-involute gear over the entire tooth width [14]. Song investigated the pitch cone based geometry design, contact characteristic analysis and dynamic analysis for external beveloid gears with parallel, intersected and crossed axes [15–17]. In aspect of external beveloid gears manufacturing, Mitome proposed the table sliding taper hobbing method for external beveloid gears and an imaginary generating planar rack cutter for the hobbing was discussed as shown in Fig. 1 [18,19]. For internal beveloid gear manufacturing, Liu derived the mathematical model of internal straight beveloid gear a shaping machine by inclining the shaper-arbor with respect to the gear axis as shown in Fig. 2 [20]. Then, tooth contact analysis was performed to investigate the transmission errors with different design parameters and assembly conditions for the internal beveloid gear pair [2]. However, due to the existing of the inclining angle between the cutters axes and the gear blank axes for the mentioned two manufacturing methods, the tilt deviations are introduced unavoidably which can affect the precise of the beveloid gear tooth profile and lead to the tooth surface profile deviations.

In this paper, the straight internal beveloid gear pair was selected as the research object. A new shaping method with parallel axes between the shaper cutter and the gear blank was proposed. And, the mathematical model of external and internal beveloid gears were derived. Then, a finite element mesh model was established and the loaded tooth contact analysis were conducted to investigate the contact characteristics for the internal beveloid gear pair. Results can provide guidance for the design and manufacturing for internal beveloid gear pairs.

2. The manufacturing and mathematical models of internal beveloid gear pair

The schematic view of the proposed manufacturing method by shaper cutter is shown in Fig. 3. The transverse sections of the shaper cutter and the gear blank parallel with each other. The shaper and the gear blank perform rotation between parallel axes with angular velocities ω_c and ω_g, respectively. The cutting motions of shaper cutter are represented using three degrees of freedom that are the rotation along its axes, translations along the axial and radial directions. DOF-1 and

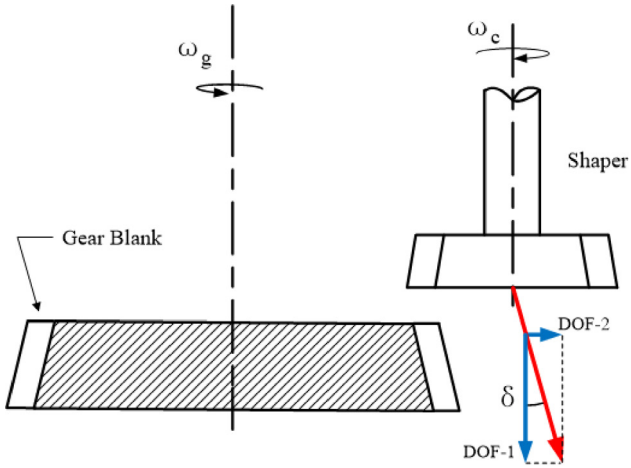

(a) External beveloid gear

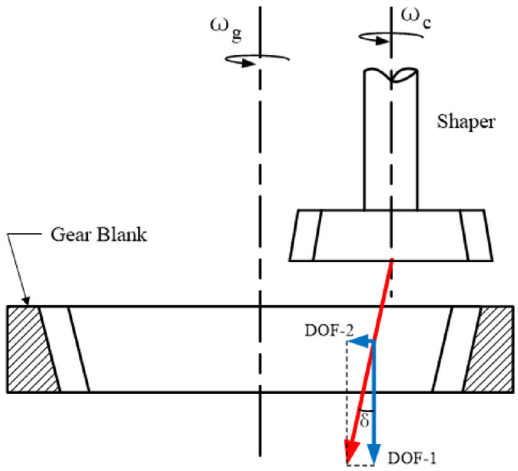

(b) Internal beveloid gear

Fig. 3. Schematic view of the cutting mechanism of beveloid gears.

DOF-2 represent the translations along the axial and radial directions, respectively. The mentioned two translations form an angle δ.

Fig. 4 illustrates the normal section of the involute shaper cutter expressed in coordinate system $O_cX_c^1Y_c^1$ and $O_cX_c^2Y_c^2$, whose origins are located in the center of the base circle. The Y_c^1 and Y_c^2 axes are located in the middle of the tooth space and tooth, respectively. Since the cutting edge of shaper cutter is symmetrical, only the left side is shown. The single tooth profile is divided into three segments $\overline{AB}$, $\overline{BC}$ and $\overline{CD}$, which are involute segment, transition arc segment and addendum arc segment, respectively. r_b and r_p are the basic circle radius and the pitch circle radius, respectively. r_c and r_{ao} are the transition arc radius of the shaper cutter and the addendum circle radius, respectively. ξ is the angle of arc between point B and point C relative to origin of the coordinate system. γ is the angle of arc $\overline{CD}\cdot\xi+\gamma$ is equivalent to $\eta-(\tan\alpha_B-\alpha_B)$ and η is equivalent to $\pi/(2z_0)+\tan\alpha-\alpha$, α is the pressure angle of pitch circle.

Segment $\overline{AB}$ of the shaper cutter is used for generating the involute surface of the beveloid gear. Parameter α_K denotes the pressure angle of arbitrary point in the involute. The segment $\overline{AB}$ can be represented in coordinate system $S_c(X_c, Y_c)$ by

$$\begin{bmatrix} X_c^1 \\ Y_c^1 \end{bmatrix} = \begin{bmatrix} \mp\frac{r_b}{\cos\alpha_k}\sin\left(\tan\alpha_k-\alpha_k-\eta+\frac{\pi}{z_0}\right) \\ \frac{r_b}{\cos\alpha_k}\cos\left(\tan\alpha_k-\alpha_k-\eta+\frac{\pi}{z_0}\right) \end{bmatrix}, \quad 0<\alpha_k<\alpha_B \tag{1}$$

$$\begin{bmatrix} X_c^2 \\ Y_c^2 \end{bmatrix} = \begin{bmatrix} \pm\frac{r_b}{\cos\alpha_k}\sin\left(\tan\alpha_k-\alpha_k-\eta\right) \\ \frac{r_b}{\cos\alpha_k}\cos\left(\tan\alpha_k-\alpha_k-\eta\right) \end{bmatrix}, \quad 0<\alpha_k<\alpha_B \tag{2}$$

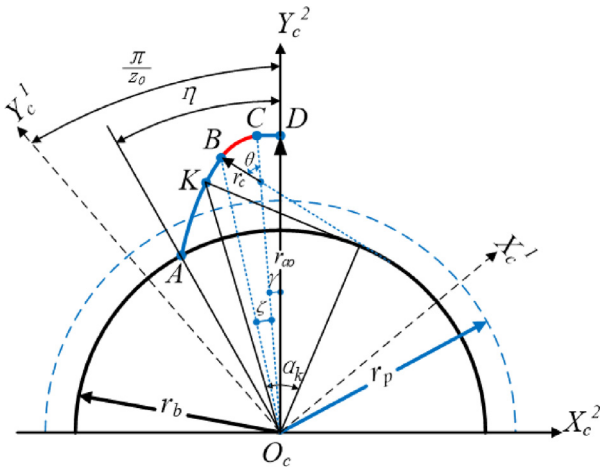

Fig. 4. The tooth profile of shaper cutter.

where the superscripts 1 and 2 denote the cutting edge in coordinate system $S_c(X_c^1, Y_c^1)$ and $S_c(X_c^2, Y_c^2)$, respectively. z_0 is the teeth number of shaper cutter, α_B is the pressure angle of the involute top endpoint and it can be determined by avoiding transition interference.

Segment $\overline{BC}$ of the shaper cutter is used to generate the transition surface of the beveloid gear. Parameter θ denotes the radian angle from point B to one point on arc $\overline{BC}$. The position vector of the point can be represented in coordinate system $S_c(X_c, Y_c)$ by

$$\begin{bmatrix} X_c^1 \\ Y_c^1 \end{bmatrix} = \begin{bmatrix} \pm r_p \cos\left(\alpha_B - (\xi+\gamma) + \theta + \frac{\pi}{z_0}\right) \pm (r_{ao} - r_c)\sin\left(\gamma - \frac{\pi}{z_0}\right) \\ r_p \sin\left(\alpha_B - (\xi+\gamma) + \theta + \frac{\pi}{z_0}\right) + (r_{ao} - r_c)\sin\left(\gamma - \frac{\pi}{z_0}\right) \end{bmatrix}, 0 < \theta < \frac{\pi}{2} - (\alpha_B - \xi) \tag{3}$$

$$\begin{bmatrix} X_c^2 \\ Y_c^2 \end{bmatrix} = \begin{bmatrix} \mp r_p \cos(\alpha_B - (\xi+\gamma) + \theta) \mp (r_{ao} - r_c)\sin\gamma \\ r_p \sin(\alpha_B - (\xi+\gamma) + \theta) + (r_{ao} - r_c)\sin\gamma \end{bmatrix}, 0 < \theta < \frac{\pi}{2} - (\alpha_B - \xi) \tag{4}$$

Addendum arc $\overline{CD}$ is used to generate the root surface of beveloid gears. As shown in Fig. 4, addendum arc $\overline{CD}$ can be represented in coordinate system $S_c(X_c, Y_c)$ by

$$\begin{bmatrix} X_c^1 \\ Y_c^1 \end{bmatrix} = \begin{bmatrix} \mp r_{ao} \sin\left(\lambda + \frac{\pi}{z_0}\right) \\ r_{ao} \cos\left(\lambda + \frac{\pi}{z_0}\right) \end{bmatrix}, -\gamma < \lambda < 0 \tag{5}$$

$$\begin{bmatrix} X_c^2 \\ Y_c^2 \end{bmatrix} = \begin{bmatrix} \mp r_{ao} \sin\lambda \\ r_{ao} \cos\lambda \end{bmatrix}, -\gamma < \lambda < 0 \tag{6}$$

where λ is the curvilinear parameter of the segment $\overline{CD}$. λ denotes the radian angle from point C to one point on arc $\overline{CD}$.

According to the cutting mechanism shown in Fig. 3, the coordinate systems between the shaper cutter and the generated gear during the generating process can be depicted in Fig. 5(a) for external beveloid gear and Fig. 5(b) for internal beveloid gear.

As shown in Fig. 5, three typical positions for the shaper cutter are defined as the upper layer, the middle layer and the lower layer. For the middle layer, the pitch circles of the shaper cutter and the beveloid gear blank are tangent to each other with the profile shift coefficient as zero. For upper layer position, the profile shift coefficient is negative for external beveloid gear (positive for internal beveloid gear). For lower layer position, the profile shift coefficient is positive for external beveloid gear (negative for internal beveloid gear). Coordinate $S_s(X_s, Y_s, Z_s)$ is fixed to the frame. Coordinate $S_t(X_t, Y_t, Z_t)$ is fixed to the pitch circle center of the shaper cutter with only the translational freedom along the cutting direction. $S_c(X_c, Y_c, Z_c)$ is fixed to the shaper cutter and represents the shaper cutter normal section. $S_f(X_f, Y_f, Z_f)$ is fixed to the frame and $S_f(X_f, Y_f, Z_f)$ is fixed to the beveloid gear blank.

For the cutting process, when the shaper cutter rotates with angle $\Delta\varphi_c$, the related rotating angle of the beveloid gear blank is $\Delta\varphi_g$. The angular velocities, rotational angle and the teeth number are related as follows

$$\frac{\omega_c}{\omega_g} = \frac{\Delta\varphi_c}{\Delta\varphi_g} = \frac{z_g}{z_c} \tag{7}$$

Fig. 6 illustrates the envelope process in arbitrary cross section of beveloid gears in one cutting motion with shaper cutter.

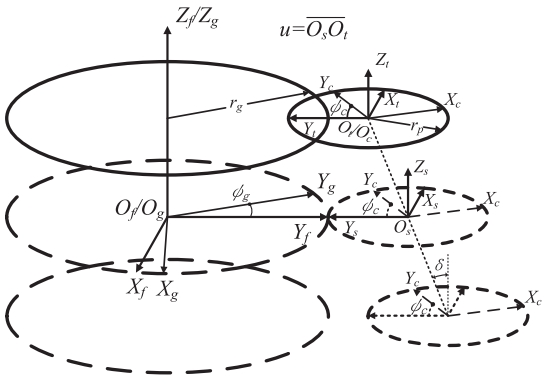

(a) External beveloid gear

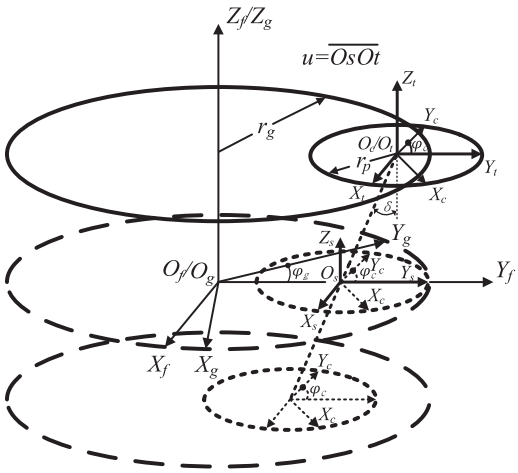

(b) Internal beveloid gear

Fig. 5. Coordination relationship between the shaper cutter and generated gear.

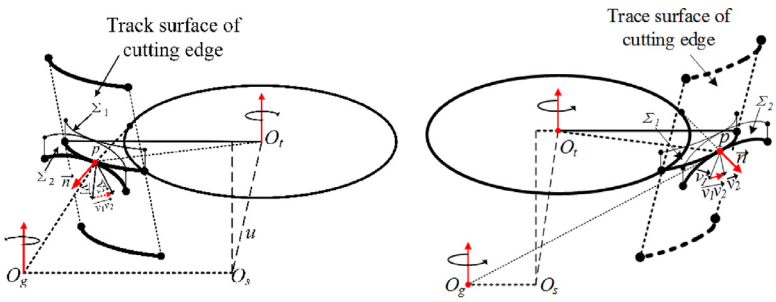

(a) External beveloid gear (b) Internal beveloid gear

Fig. 6. The envelope surface of the shaper cutter for beveloid gear.

The cutting edge of the shaper cutter formed a trace surface in its cutting path, and the tooth profile of the shaper cutter creates involute profile on each transverse sections of the beveloid gear. In order to describe the envelope surfaces, the cutting edge and the generated profile curve of beveloid gear are swept along their axes to form micro surface Σ_1 and Σ_2, respectively. The micro surface Σ_1 can be described as $\Sigma_1 = h(L, t)$, where L is the curvilinear parameter of the cutting edge (L is represented by α_K,θ,λ in segment $\overline{AB}$, $\overline{BC}$, $\overline{CD}$ respectively), t is the sweep length (When t is equal to zero, the surface equation of Σ_1 turns into the equations of segment $\overline{AB}$, $\overline{BC}$ and $\overline{CD}$). According to the gear meshing theory, the micro surface Σ_1 and Σ_2 should be tangent at the contact point P, during the generating process. $\vec{v_1}$ and $\vec{v_2}$ are the velocity of

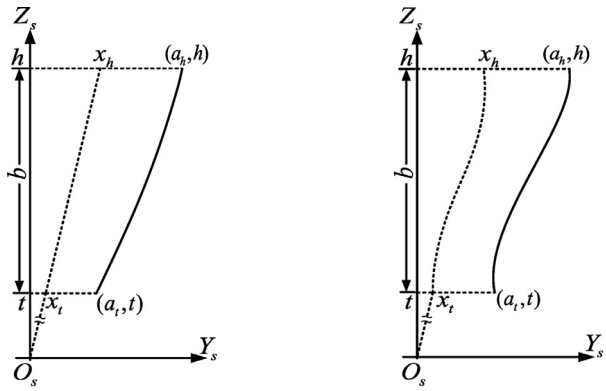

(a) Linear profile shift coefficient (b) Nonlinear profile shift coefficient

Fig. 7. The cutting path of shaper cutter.

shaper cutter and the beveloid gears at point P. $\overrightarrow{v_1v_2}$ is the relative velocity and $\overrightarrow{n}$ is the common normal vector of the two micro surface at point P. Considering the transformation matrix from S_c to S_t, the micro surface Σ_1 can be represented in coordinate system S_t by

$$R_t^1 = \begin{bmatrix} X_t \\ Y_t \\ Z_t \end{bmatrix} = \begin{bmatrix} X_c^1 \cos\varphi_c + Y_c^1 \sin\varphi_c \\ -X_c^1 \sin\varphi_c + Y_c^1 \cos\varphi_c \\ t \end{bmatrix} \tag{8.a}$$

$$R_t^2 = \begin{bmatrix} X_t \\ Y_t \\ Z_t \end{bmatrix} = \begin{bmatrix} X_c^2 \cos\varphi_c - Y_c^2 \sin\varphi_c \\ X_c^2 \sin\varphi_c + Y_c^2 \cos\varphi_c \\ t \end{bmatrix} \tag{8.b}$$

where the superscripts 1 and 2 refer to the external and internal beveloid gear, respectively.

The unit normal vector to the micro surface Σ_1 can be calculated by

$$\mathbf{n_t} = \frac{\partial R_t}{\partial L} \times \frac{\partial R_t}{\partial L} = \begin{vmatrix} \mathbf{i} & \mathbf{j} & \mathbf{k} \\ \frac{\partial X_t}{\partial L} & \frac{\partial Y_t}{\partial L} & \frac{\partial Z_t}{\partial L} \\ \frac{\partial X_t}{\partial t} & \frac{\partial Y_t}{\partial t} & \frac{\partial Z_t}{\partial t} \end{vmatrix} = n_{xt}\mathbf{i} + n_{yt}\mathbf{j} + n_{zt}\mathbf{k} \tag{9}$$

The trajectory curves of the shaper cutter during the cutting process are depicted in Fig. 7. The equation of cutting path can be described as $g(Y_s, Z_s) = 0$ with parameters Y_s, Z_s in coordinate system S_s. When the parameters Y_s and Z_s meet the following relationship (10) and (11), the generated beveloid gear with a linear variable profile shift coefficient can be processed. When the parameters Y_s and Z_s meet any other curve equations, beveloid gears with a nonlinear variable profile shift coefficient can be generated.

$$\begin{bmatrix} Y_s \\ Z_s \end{bmatrix} = \begin{bmatrix} \frac{m(z_{1,2} \pm z_0)}{2} \cdot \frac{\cos\alpha}{\cos\alpha_{0(1,2)}} \\ \frac{b}{x_h - x_t} \cdot (x_{1,2} - x_t) \end{bmatrix}, \; x_t \le x_{1,2} \le x_h, \tag{10}$$

$$inv\alpha_{0(1,2)} = \frac{2x_{1,2}}{z_{1,2} \pm z_0} + inv\alpha \tag{11}$$

where $x_{1,2}$ is the profile shift coefficient of external or internal beveloid gear, $\alpha_{0(1,2)}$ is the meshing angle when external or internal beveloid gear processed by shaper cutter, the upper symbol '+' and lower symbol '-' work for the external and internal beveloid gear, respectively.

Based on the homogeneous coordinate transformation from S_t to S_s, The transformation matrix M_{st} and L_{st} can be written as follows.

$$M_{st} = \begin{bmatrix} 1 & 0 & 0 & 0 \\ 0 & 1 & 0 & u\sin\delta \\ 0 & 0 & 1 & u\cos\delta \\ 0 & 0 & 0 & 1 \end{bmatrix} \tag{12}$$

Table 1
Major design parameters of the internal beveloid gear pair.

Parameters	External beveloid gear	Internal beveloid gear
Module (mm)	$m = 2.5$	
Pressure angle (°)	$\alpha = 20$	
Meshing angle (°)	$\alpha' = 26$	
Center distance (mm)	$a = 19.6032$	
Tooth numbers of shaper cutter	$Z_0 = 30$	
Tooth numbers of beveloid gears	$Z_1 = 45$	$Z_2 = 60$
Tooth width (mm)	$b_1 = 22.5$	$b_2 = 22.5$
Modification coefficient increasing along axis	x_1 : 0.9 → 1.78	x_2 : 1.29239334 → 2.17239334

$$L_{st} = \begin{bmatrix} 1 & 0 & 0 \\ 0 & 1 & 0 \\ 0 & 0 & 1 \end{bmatrix} \tag{13}$$

For the meshing during the generating process, the micro surface Σ_1 of the cutter shaper and Σ_2 of the external beveloid gear (or internal beveloid gear) should be in continuous tangency. The equation of meshing can be determined in coordinate system S_s as

$$f(L, \varphi_c, g(u, \delta)) = \mathbf{n_s} \times \mathbf{v_1 v_2}^{(s)} = L_{st} \cdot n_t \times \mathbf{v_1 v_2}^{(s)} = 0 \tag{14}$$

where the subscript s indicates that the vector is expressed in coordinate S_s. $\mathbf{v_1 v_2}^{(s)}$can be represented by

$$\mathbf{v_1 v_2}^{(s)} = \mathbf{v_2}^{(s)} - \mathbf{v_1}^{(s)} = \mathbf{O_g P}^{(s)} \times \boldsymbol{\omega_g}^{(s)} - \mathbf{O_t P}^{(s)} \times \boldsymbol{\omega_c}^{(s)} \tag{15}$$

where $\mathbf{O_g P}^{(s)}$ denotes the distance between $\mathbf{O_g}^{(s)}$ and $\mathbf{P}^{(s)}$, $\mathbf{O}_t\mathbf{P}^{(s)}$ denotes the distance between $\mathbf{O}_t^{(s)}$ and $\mathbf{P}^{(s)}$. $\boldsymbol{\omega_g}^{(s)}$ and $\boldsymbol{\omega_c}^{(s)}$ represent the generating motions rotated around the beveloid gear blank and shaper cutter axes, respectively.

The coordinate transformation matrixes for the transferring from S_s to S_f and S_f to S_g can be obtained as

$$M_{fs}^1 = \begin{bmatrix} 1 & 0 & 0 & 0 \\ 0 & 1 & 0 & r_g + r_p \\ 0 & 0 & 1 & 0 \\ 0 & 0 & 0 & 1 \end{bmatrix} \tag{16}$$

$$M_{fs}^2 = \begin{bmatrix} 1 & 0 & 0 & 0 \\ 0 & 1 & 0 & r_g - r_p \\ 0 & 0 & 1 & 0 \\ 0 & 0 & 0 & 1 \end{bmatrix} \tag{17}$$

$$M_{gf}^1 = \begin{bmatrix} \cos\varphi_g & -\sin\varphi_g & 0 & 0 \\ \sin\varphi_g & \cos\varphi_g & 0 & 0 \\ 0 & 0 & 1 & 0 \\ 0 & 0 & 0 & 1 \end{bmatrix} \tag{18}$$

$$M_{gf}^2 = \begin{bmatrix} \cos\varphi_g & \sin\varphi_g & 0 & 0 \\ -\sin\varphi_g & \cos\varphi_g & 0 & 0 \\ 0 & 0 & 1 & 0 \\ 0 & 0 & 0 & 1 \end{bmatrix} \tag{19}$$

Then the position vector of the point can be represented in coordinate system S_g as follows

$$\mathbf{R}_g = \begin{bmatrix} X_g \\ Y_g \\ Z_g \end{bmatrix} = M_{gf} M_{fs} M_{st} \mathbf{R}_t, \ (t = 0) \tag{20}$$

Based on above equations, the tooth-surface equation of external beveloid gear can be derived in coordinate system S_g as

$$\mathbf{R}_g = \begin{bmatrix} X_g \\ Y_g \\ Z_g \end{bmatrix} = \begin{bmatrix} X_c \cos(\varphi_c - \varphi_g) + Y_c \sin(\varphi_c - \varphi_g) - (u \sin\delta + r_g + r_p) \sin\varphi_g \\ -X_c \sin(\varphi_c - \varphi_g) + Y_c \cos(\varphi_c - \varphi_g) + (u \sin\delta + r_g + r_p) \cos\varphi_g \\ u \cos\delta \end{bmatrix} \tag{21}$$

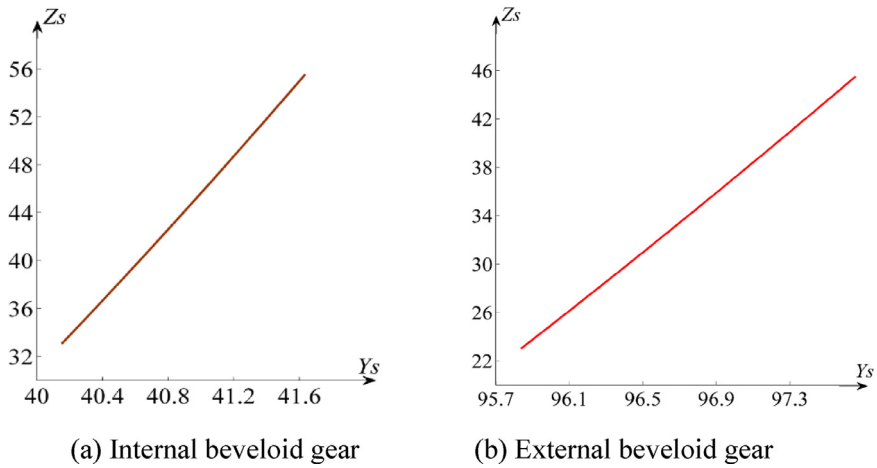

Fig. 8. The cutting path for the internal beveloid gear pair.

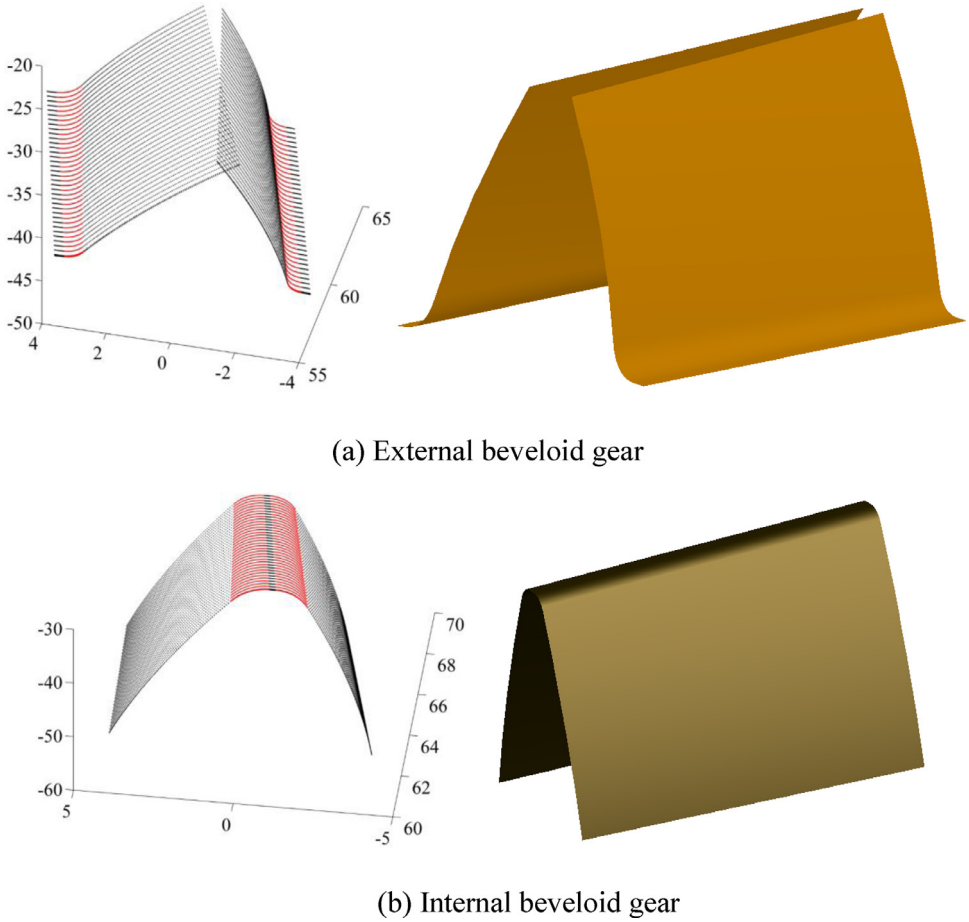

Fig. 9. The tooth surface model of beveloid gear.

Similarly, the tooth-surface of internal beveloid gear can be expressed in coordinate system S_g as follows

$$\mathbf{R}_g = \begin{bmatrix} X_g \\ Y_g \\ Z_g \end{bmatrix} = \begin{bmatrix} X_c \cos(\varphi_c - \varphi_g) - Y_c \sin(\varphi_c - \varphi_g) + (u \sin\delta + r_g - r_p) \sin\varphi_g \\ X_c \sin(\varphi_c - \varphi_g) + Y_c \cos(\varphi_c - \varphi_g) + (u \sin\delta + r_g - r_p) \cos\varphi_g \\ u \cos\delta \end{bmatrix} \tag{22}$$

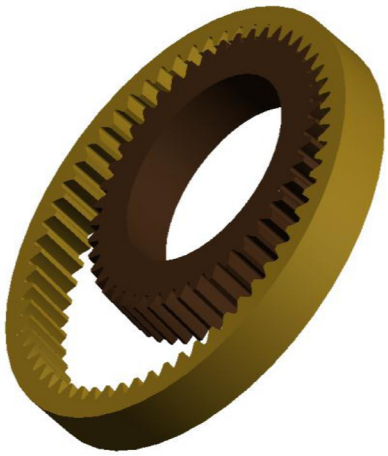

Fig. 10. The assembly model.

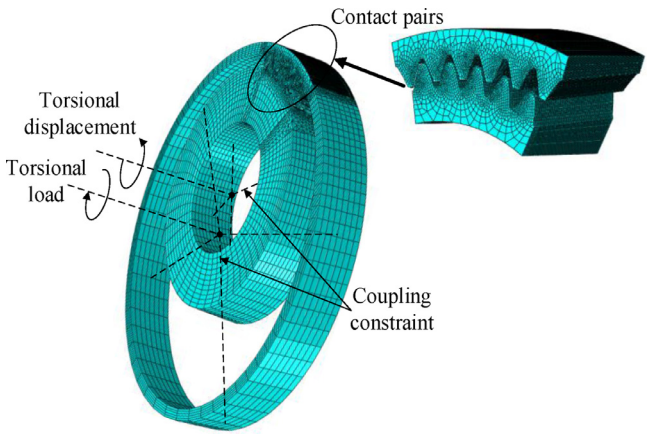

Fig. 11. The FE model.

3. Mesh model of internal beveloid gear pair

A pair of internal beveloid gears was used to investigate the contact characteristics. The gear geometry design parameters for the external and internal beveloid gears are listed in Table 1.

To obtain the internal beveloid gear pair with linear variable profile shift coefficient, the cutting path as a curve was used as shown in Fig. 8.

The generating procedure was programed using commercial calculation software Matlab. Then the coordinates of the points on the beveloid gear tooth surface were calculated and imported into a CAD software to generate the beveloid gear tooth surface. The calculated points coordinates and tooth surface models for external and internal beveloid gears are shown in Fig. 9.

Based on the tooth surface model of beveloid gears defined by the geometrical parameters given in Table 1, the three dimensional solid assembly model was created as shown in Fig. 10. Then the model was imported to a commercial FEM software Abaqus and the mesh discretization for the internal beveloid gear pair was carried out. The finite element assembly model is shown in Fig. 11.

For the loaded mesh model of the internal beveloid gear pair, the material property, mesh settings and boundary conditions were defined as follow:

(1) Material used for the model is 17CrNiMo6. The young's modulus is 208,000 Mpa, and the Poisson's ratio is 0.298. Material property is isotropic.
(2) For the internal beveloid gear pair, 5 teeth for each gear were considered to reduce the computing cost. The FE model of external and internal beveloid gear has 218,192 and 170,085 elements respectively.

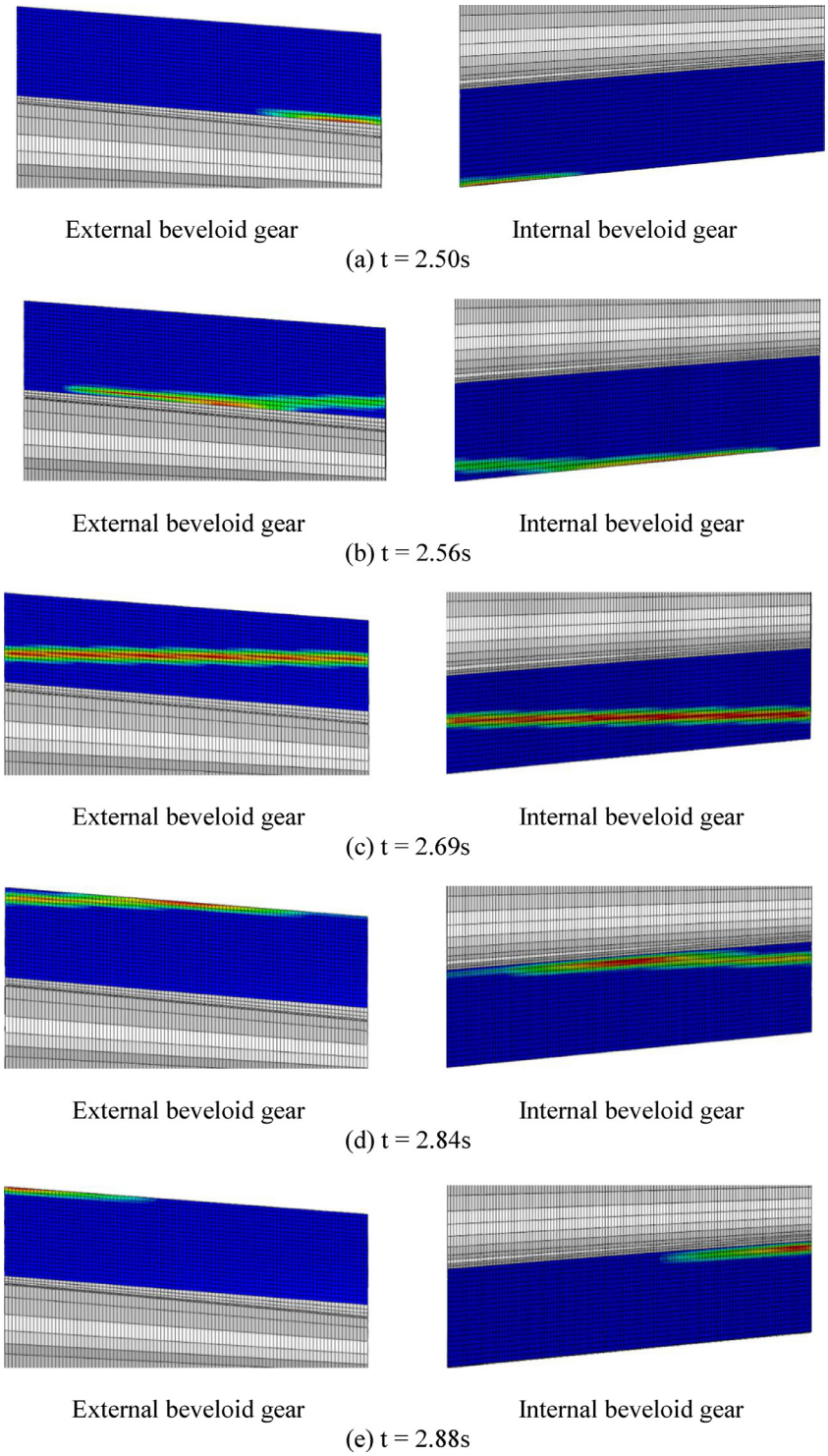

Fig. 12. The tooth mesh condition of beveloid gear.

(3) The surface to surface contact interactions were created between the teeth of the external beveloid gear and the related teeth of the internal beveloid gear.
(4) The kinematic couplings with 6 degrees of freedom were created between the center points and the surfaces of the gear wholes to set the boundary constraints. Then, Torsional displacement was applied to the external beveloid gear as the input for the loaded tooth contact analysis and torque load was applied to the internal beveloid gear as the output.

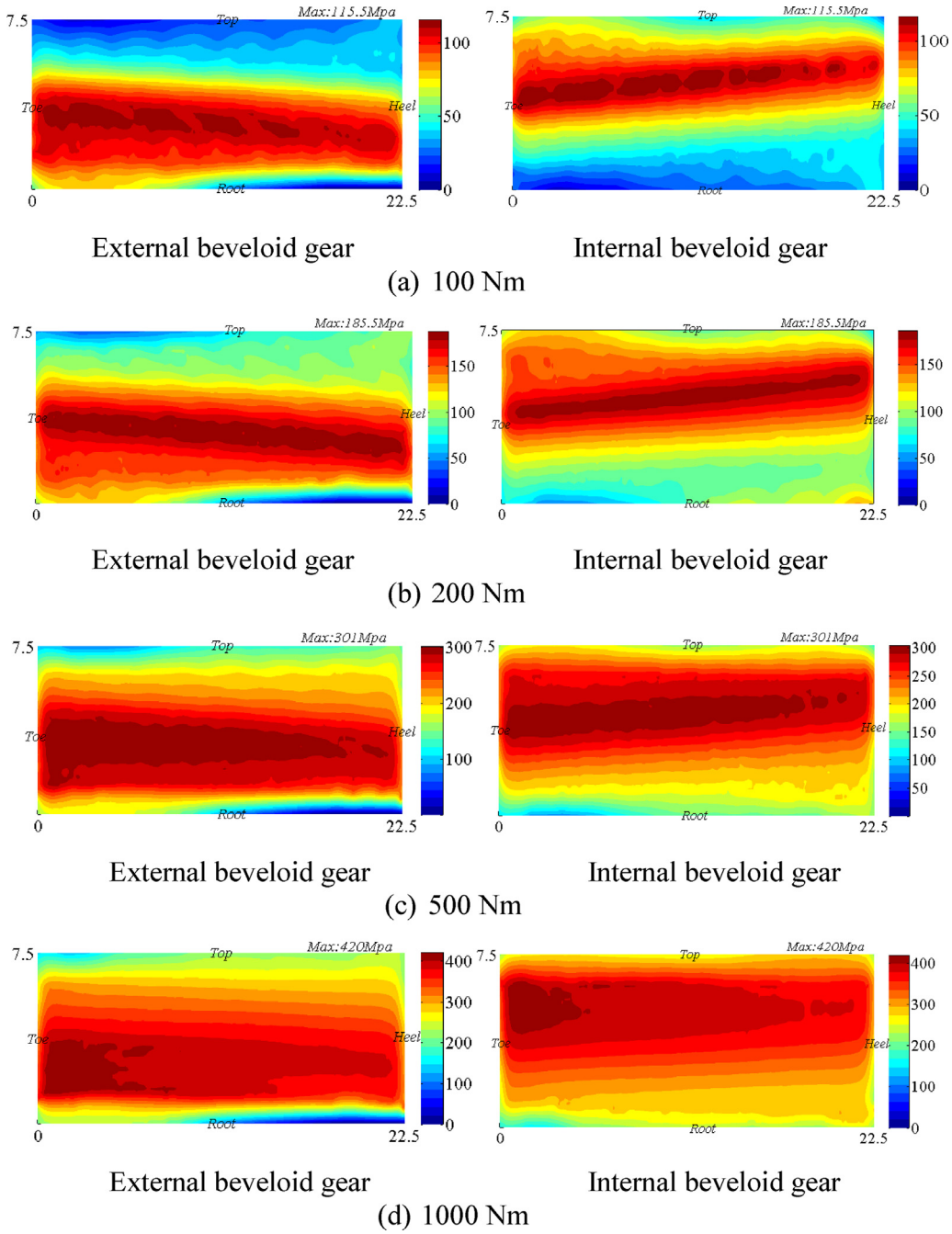

Fig. 13. The tooth contact pattern.

4. Contact characteristics analysis

Fig. 12.a–e show the tooth contact results for different engagement moments under a torque load 200 Nm.

It can be seen that the tooth meshes in at the toe and meshes out at the heel. An obvious line contact type can be found during the meshing for the internal beveloid gear pair and the simultaneous contact line is parallel to the axes of beveloid gears. This is different from the point contact for the crossed and intersected beveloid gears from the previous research [8,9,21]. For the whole mesh cycle, the length of the simultaneous contact line on tooth surface increases first and then decreases due to the cone angle. Also, the maximum length of the simultaneous contact line is equal to the tooth width.

Fig. 13 shows the tooth contact pattern of the internal beveloid gear pair under 100 Nm, 200 Nm, 500 Nm, and 1000 Nm torque load levels, respectively. It can be seen that the tooth contact pattern distributes in the middle the tooth surface

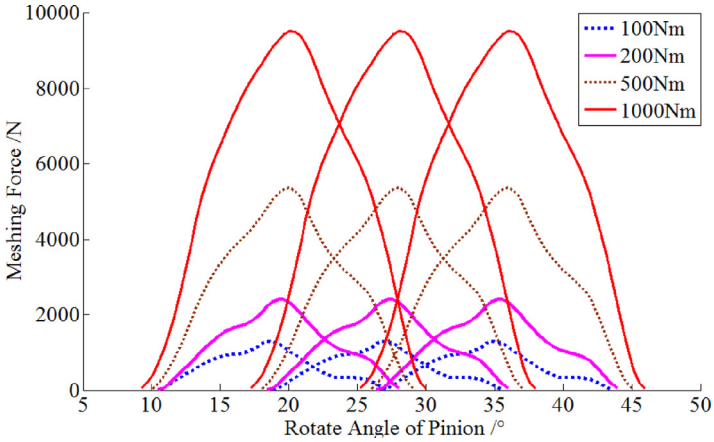

Fig. 14. The meshing force of internal beveloid gear pair.

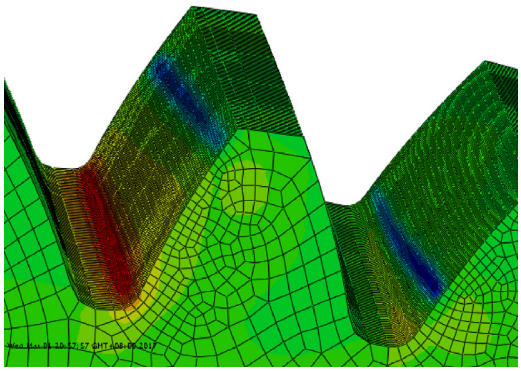

Fig. 15. The root bending stress distribution of external beveloid gear.

along the tooth width direction and tooth profile direction. The increase of the torque load from 100 Nm to 1000 Nm tends to increase the area of the contact pattern up to about 95% of the tooth surface. Also, the maximum contact pressure was increased from 115.5 Mpa to 420 Mpa.

The time-varying meshing forces of internal beveloid gear pair with different torque loads are shown in Fig. 14. It can be seen that the gear pair mesh smoothly without any sudden peaks and the increase of the torque load tends to increase the mesh force gradually. Also, the contact ratio is not a constant but a varying value from about 2 to 3 with the increase of the torque load. With a light load level 100 Nm, the contact ratio is about 2. However, it was increased to a larger value between 2 and 3 with the torque load increased to 500 Nm and 1000 Nm due to contact deformation and the elastic deformation of the teeth.

The root bending stress distribution of external beveloid gear under 500 Nm load case is shown in Fig. 15. And the root bending stresses along tooth width direction in a mesh cycle are shown in Fig. 16. From the results, the root stresses are almost as a line. For the meshing in process from 0.47 s to 0.70 s, the largest value of the root stress is located in the toe. However, for the meshing out process from 0.8 s to 0.9 s, the largest value of the root stress is shifted to the heel.

Fig. 17 show the time-varying and peak-peak value of the static angular transmission error. The time-varying and the mean value of the mesh stiffness results are shown in Fig. 18. From the results, the angular transmission errors are obviously parabolic in shape and the increase of torque load tends to increase the peak-peak value of angular transmission error. But the increase tendency of peak-peak value reduces. The shape of the mesh stiffness becomes smoother as the load increases due to more area coming into contact. And the mean value of the mesh stiffness becomes larger.

5. Conclusions

In this paper, the generation method with a shaper cutter for the straight internal beveloid gear pair was investigated and the contact characteristics of the gear pair were analyzed. Based on the calculated results, the following specific conclusions can be obtained.

(1) A new shaping method with parallel axes between the shaper cutter and the gear blank was proposed. The cutting motion of shaper cutter is represented using three degrees of freedom that are the rotation along its axes, transla-

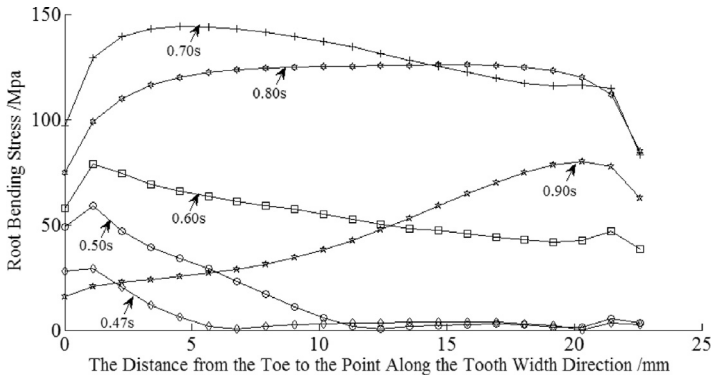

Fig. 16. The root bending stress along tooth width direction in a mesh cycle.

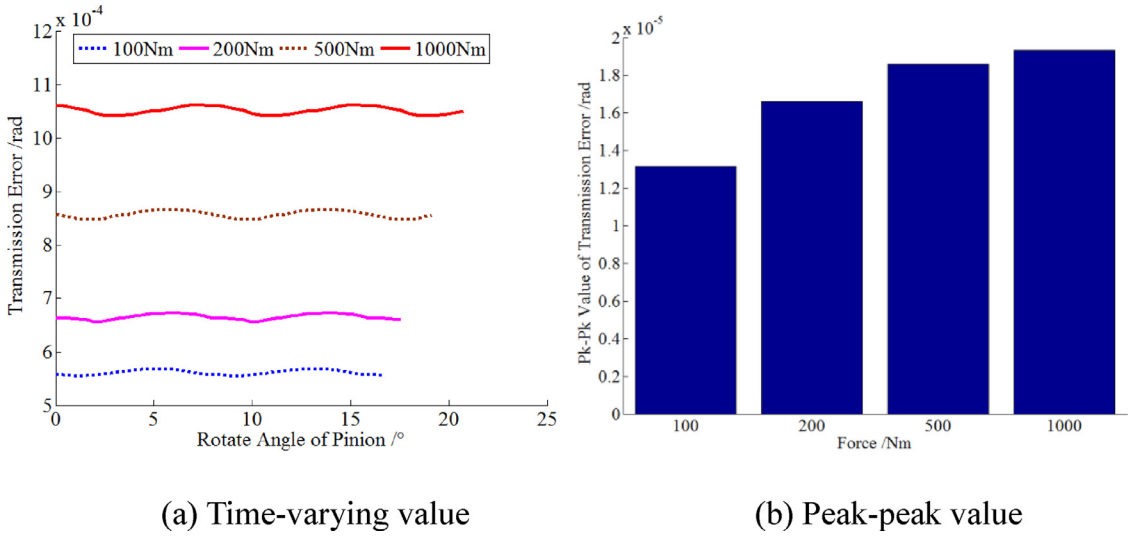

Fig. 17. Effects of load on angular transmission error.

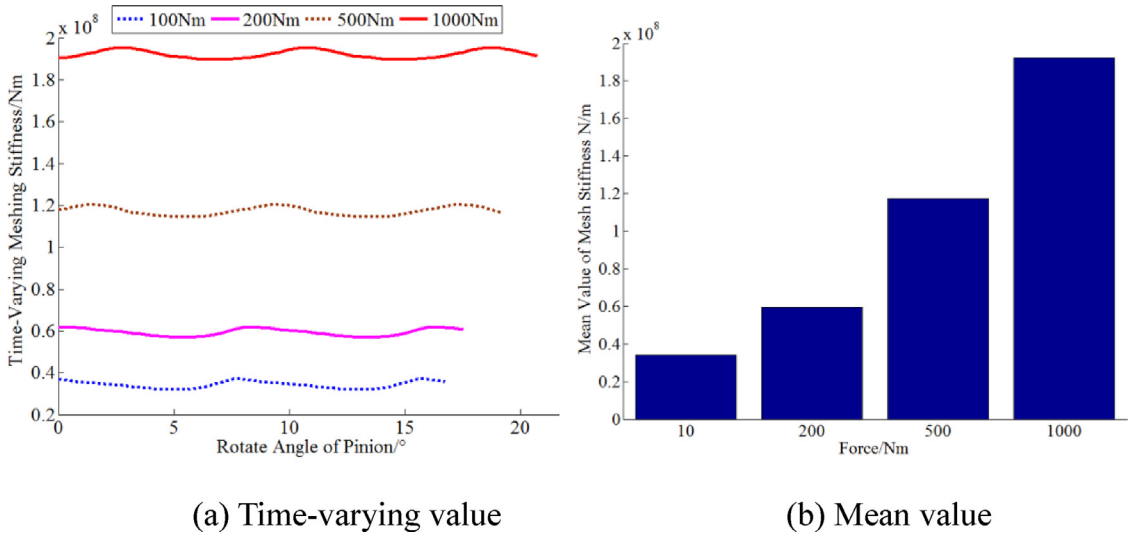

Fig. 18. Effects of load on mesh stiffness.

tions along the axial and radial directions. With the proposed method, the beveloid gear with a linear or nonlinear variable profile shift coefficient along the tooth width direction can be generated and the tilt deviations due to the conventional inclined cutting tool shaft can be avoided.

(2) Compared with the cylindrical spur gear pair, the tooth meshes in at the toe and meshes out at the heel for the straight internal beveloid gear pair. And, the length of the simultaneous contact line on tooth surface increases first and then decreases due to the cone angle.

(3) As the torque load increases, the mesh area, contact pressure on the tooth surface, mean value of mesh stiffness and the peak-peak value of angular transmission error are increased due to the elastic deformation of the gear pair. However, the speed of the increase tendency slows down.

Acknowledgments

The authors would like to thank the National Natural Science Foundation of China (Grant No. 51405043, No. 51575060 and No. 51575061), China Postdoctoral Science Foundation (Grant No. 2015M582517 and No. 2015M590861), Chongqing Research Program of Basic Research and Frontier Technology (No. cstc2016jcyjA0415), Postdoctoral Special Projects Funded of Chongqing (No. Xm2016004) and Prof. Teik C. Lim (College of Engineering and Applied Science at the University of Cincinnati.).

References

[1] H.E. Merritt, Gears, third ed., Isaac Pitman & Sons, 1954.
[2] C.-C. Liu, S.F. Wang, Tooth contact analysis and contact ellipse simulation of internal conical gear pairs, in: 12th IFToMM World Congress, 2007, pp. 18–21.
[3] K. Mitome, T. Yamazaki, Design of conical involute gear engaged with profile spur gear on intersecting shafts (in Japanese), Trans. Hapan Soc. Mech. Eng. Part C 62 (598) (1996) 2436–2441.
[4] J. Brauer, Transmission error in anti-backlash conical involute gear transmissions: a global–local fe approach, Finite Elem. Anal. Des. 41 (2005) 431–457.
[5] C.-C. Liu, C.-B. Tsay, Contact characteristics of beveloid gears, Mech. Mach. Theory 37 (2002) 333–350.
[6] S.J. Tsai, S.-H. Wu, Geometrical design of conical gear drives with profile-shifted transmission, 12th IFToMM World Congress, Besançon (France), 2007, June, 18-21.
[7] L. Guixian, W. Jianmin, Z. Xin, L. Yu, Meshing theory and simulation of noninvolute beveloid gears, Mech. Mach. Theory 39 (8) (2004) 883–892.
[8] C. Song, C. Zhu, W. Liu, Sliding friction effect on dynamics of crossed beveloid gears with small shaft angle, J. Mech. Sci. Technol. 27 (5) (2013) 1255–1263.
[9] C. Song, C. Zhu, T.C. Lim, T. Peng, Parametric analysis of gear mesh and dynamic response of loaded helical beveloid transmission with small shaft angle, J. Mech. Des. 134 (8) (2012) 1–8.
[10] K. Mitome, Conical involute gear (design of nonintersecting-nonparallel-axis conical involute gear), JSME Int. J. Ser. III 34 (2) (1991) 265–270.
[11] J. Brauer, Analytical geometry of straight conical involute gears, Mech. Mach. Theory 37 (1) (2002) 127–141.
[12] S.H. Wu, S.J. Tsai, Geometrical design of skew conical involute gear drives in approximate line contact, Proc. Inst. Mech. Eng. Part C J. Mech. Eng. Sci. 223 (9) (2009) 2201–2211.
[13] S.H. Wu, S.J. Tsai, Contact stress analysis of skew conical involute gear drives in approximate line contact, Mech. Mach. Theory 44 (9) (2009) 1658–1676.
[14] Kohei Hori, Iwao Hayashi, Nobuyuki Iwatsuki, The ideal tooth profiles of conical-external and -internal gears meshing with cylindrical-involute gears over the entire tooth width, JSME Int. J. Ser. C 41 (4) (1998) 901–911.
[15] G. Ni, C. Zhu, C. Song, H. Liu, Geometric design and meshing characteristics analysis of beveloid gear transmission with parallel axes, J. Xi'an Jiaotong Univ. 50 (5) (2016) 57–64.
[16] C. Zhu, L. Liu, C. Song, Y. Xiang, H. Liu, Pitch cone design and tooth contact analysis of intersected beveloid gears for marine transmission, Mech. Mach. Theory 82 (2014) 141–153.
[17] C. Song, C. Zhu, H. Liu, G. Ni., Dynamic analysis and experimental study of a marine gearbox with crossed beveloid gears, Mech. Mach. Theory 92 (2015) 17–28.
[18] K. Mitome, Table sliding taper hobbing of conical gear using cylindrical hob, part 1: theoretical analysis of table sliding taper hobbing, Trans. ASME 103 (1981) 46–451.
[19] K. Mitome, Table sliding taper hobbing of conical gear using cylindrical hob, part2: hobbing of conical involute gear, Trans. ASME 103 (1981) 542-455.
[20] C-C. Liu, The mathematical model and tooth surface deviation of internal conical gears, in: Proceedings of ASME 2005 International Design Engineering Technical Conference & Computers and Information in Engineering Conference, Long Beach, California USA, 2005 DETC2005-84097.
[21] C. Zhu, L. Liu, C. Song, Y. Xiang, H. Liu, Pitch cone design and tooth contact analysis of intersected beveloid gears for marine transmission, Mech. Mach. Theory 82 (2014) 141–153.